The EMBO Journal vol.13 no.10 pp.2452–2463, 1994

The 5′ end of yeast 5.8S rRNA is generated by exonucleases from an upstream cleavage site

Yves Henry, Heather Wood, John P.Morrissey, Elisabeth Petfalski, Stephen Kearsey[1] and David Tollervey

EMBL, Postfach 102209, 69012 Heidelberg, Germany and [1]Department of Zoology, University of Oxford, South Parks Road, Oxford OX1 3PS, UK

Communicated by A.Lamond

We have developed techniques for the detailed analysis of *cis*-acting sequences in the pre-rRNA of *Saccharomyces cerevisiae* and used these to study the processing of internal transcribed spacer 1 (ITS1) leading to the synthesis of 5.8S rRNA. As is the case for many eukaryotes, the 5′ end of yeast 5.8S rRNA is heterogeneous; we designate the major, short form 5.8S(S), and the minor form (which is seven or eight nucleotides longer) 5.8S(L). These RNAs do not have a precursor/product relationship, but result from the use of alternative processing pathways. In the major pathway, a previously unidentified processing site in ITS1, designated A3, is cleaved. A 10 nucleotide deletion at site A3 strongly inhibits processing of A3 and the synthesis of 5.8S(S); processing is predominantly transferred to the alternative 5.8S(L) pathway. Site A3 lies 76 nucleotides 5′ to the end of 5.8S(S), and acts as an entry site for 5′→3′ exonuclease digestion which generates the 5′ end of 5.8S(S). This pathway is inhibited in strains mutant for XRN1p and RAT1p. Both of these proteins have been reported to have 5′→3′ exonuclease activity *in vitro*. Formation of 5.8S(L) is increased by mutations at A3 *in cis* or in RAT1p and XRN1p *in trans*, and is kinetically faster than 5.8S(S) synthesis.

Key words: pre-rRNA processing/ribosome synthesis/ *Saccharomyces cerevisiae*

Introduction

The nuclear ribosomal DNA (rDNA) genes of all eukaryotes have the same arrangement, in which the small subunit rRNA gene (18S in yeast) and two large subunit rRNA genes (5.8S and 25S in yeast) are cotranscribed by RNA polymerase I into a large pre-ribosomal RNA (pre-rRNA) (35S pre-rRNA in yeast), which undergoes sequential cleavage to yield the mature rRNAs (see Figure 1A and B). The rRNA coding regions of all eukaryotes are flanked by the 5′ and 3′ external transcribed spacers (5′ and 3′ ETS) and separated by internal transcribed spacers 1 and 2 (ITS1 and ITS2) (see Figure 1A). The pathway by which the pre-rRNA is processed to yield the mature rRNAs has been studied for a number of eukaryotes, but is understood in most detail for the budding yeast *Saccharomyces cerevisiae*. For reasons that are not clear, the yeast rRNAs are not excised by simple cleavage at their mature ends, but are generated by a pathway involving cleavages in the 5′ ETS, 3′ ETS, ITS1 and ITS2 regions.

The earliest cleavage in the yeast 35S pre-rRNA is within the 5′ ETS at site A0 to give the 33S pre-rRNA (see Figure 1B) (Hughes and Ares, 1991), although it is not certain that this is an intermediate on the major pre-rRNA processing pathway. This is followed by cleavage at site A1, the 5′ end of the 18S rRNA, to give the 32S pre-rRNA. The next cleavage, at site A2 in ITS1, separates the 20S and 27SA pre-rRNAs, which are destined to form the small and large ribosomal subunits respectively (Udem and Warner, 1972; Veldman *et al.*, 1980, 1981). Cleavage at A2 was believed to be followed by cleavage at site B1, the 5′ end of the 5.8S rRNA, but the data reported here show that processing in this region is more complex than anticipated.

Mutations in a number of *trans*-acting factors have been shown to inhibit these pre-rRNA cleavages. Many of these are the small nucleolar RNAs (snoRNAs) which are associated with proteins in small nucleolar ribonucleoprotein particles (snoRNPs). Cleavage at site A0 requires the U3 snoRNA and the U3 snoRNP proteins NOP1p and SOF1p, but does not require other snoRNAs and snoRNP proteins tested (Hughes and Ares, 1991; D.Tollervey, unpublished). In strains depleted of one of several different snoRNP components, the snoRNAs U3, U14 and snR30, and the snoRNP proteins NOP1p, SOF1p or GAR1p, the 32S, 27SA and 20S pre-rRNAs are not synthesized, and the 18S rRNA does not accumulate (Li *et al.*, 1990; Hughes and Ares, 1991; Tollervey *et al.*, 1991; Girard *et al.*, 1992; Jansen *et al.*, 1993; Morrissey and Tollervey, 1993). In contrast, synthesis of 5.8S and 25S rRNA is little affected. This indicates that in these strains the cleavages at both A1 and A2 are inhibited (see Figure 1B). We report here that, as judged by primer extension, A2 cleavage is indeed blocked in all of these mutants. In addition, all of these strains synthesize an aberrant pre-rRNA designated 23S. Hybridization with probes specific for different regions of ITS1 shows that in all of the snoRNP mutants, the 23S pre-rRNA extends from the 5′ end of the 35S pre-rRNA to a site 3′ of site A2, but not as far as B1 (Morrissey and Tollervey, 1993) (see Figure 1). We interpreted this as showing that a previously unidentified cleavage site is located in the 3′ region of ITS1, between A2 and B1. Cleavage at this site presumably continues in the absence of A1/A2 cleavage and generates the 3′ end of the 23S pre-rRNA.

Mutations in another ribonucleoprotein complex, RNase MRP, also affect yeast pre-rRNA processing. RNase MRP was identified from vertebrates by an assay for the *in vitro* cleavage of the RNA primer for mitochondrial DNA replication (Chang and Clayton, 1987a,b). The RNA component (7-2 RNA) is, however, largely localized in the nucleolus (Reddy *et al.*, 1985; Yuan *et al.*, 1989; Kiss *et al.*,

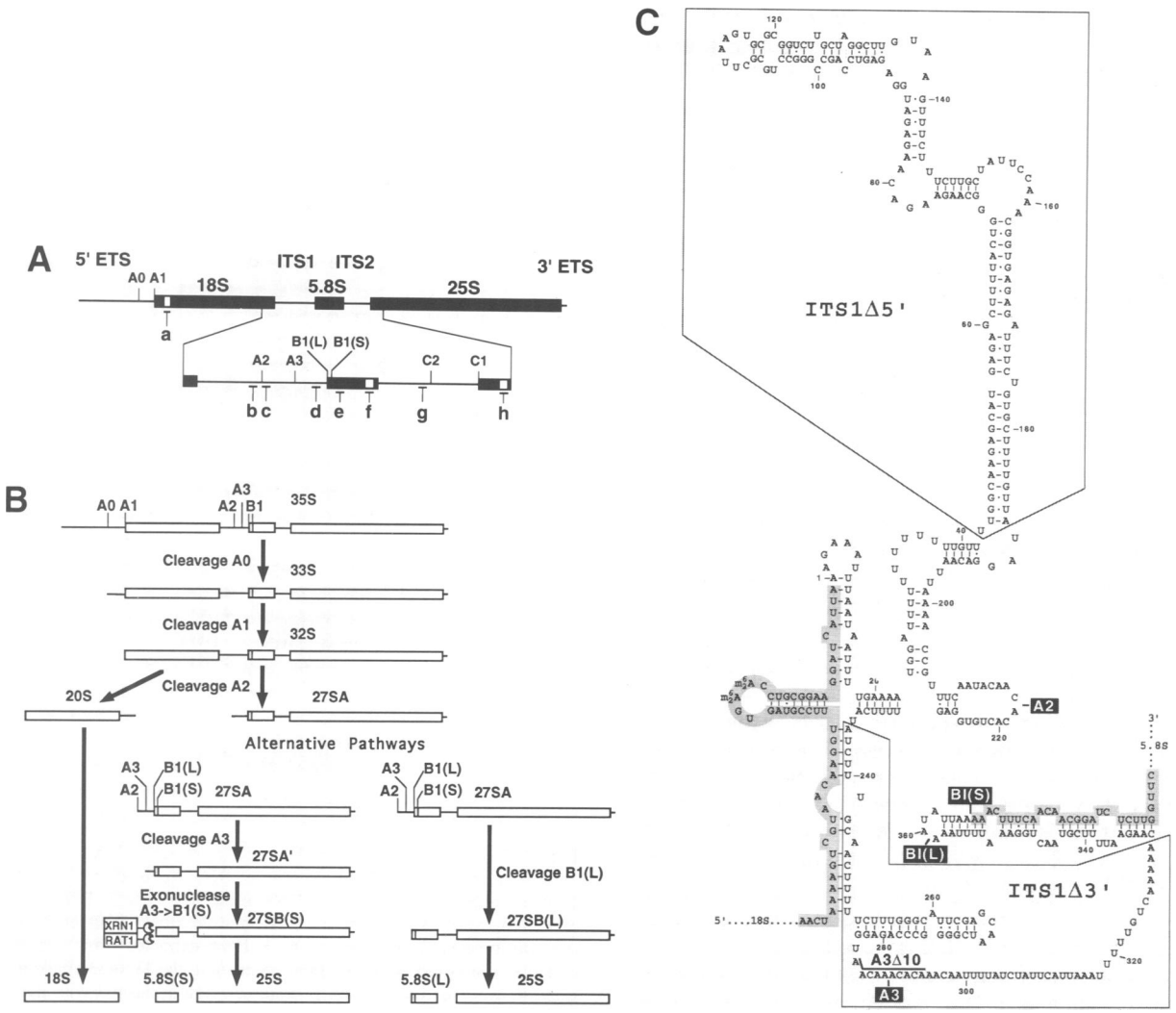

Fig. 1. Structure and processing of the yeast pre-rRNA. (**A**) Structure of 35S pre-rRNA and locations of oligonucleotides. The regions to which oligonucleotides a–h hybridize are indicated. Open boxes within the 18S, 5.8S and 25S rRNA regions indicate the locations of the tags. (**B**) The pathway of pre-rRNA processing in *Saccharomyces cerevisiae*. The rDNA is transcribed into a 35S pre-rRNA which undergoes snoRNP-dependent cleavages at site A0 in the 5′ ETS (generating the 33S pre-rRNA), site A1 at the 5′ end of the 18S rRNA (generating 32S pre-rRNA) and site A2 in ITS1 (generating the 20S and 27SA pre-rRNAs). A2 cleavage separates the pre-rRNAs destined to form the small and large ribosomal subunits. The 20S pre-rRNA is cleaved, probably endonucleolytically, to generate the 18S rRNA. The 27SA pre-rRNA can be processed by two alternative pathways. In the major pathway, 27SA is cleaved at site A3 to generate the 27SA′ pre-rRNA. A3 acts as an entry site for an exonuclease activity which requires the RAT1p and XRN1p proteins and degrades the pre-rRNA 5′→3′ to site B1(S) generating the 5′ end of the short form of the 27SB pre-rRNA, 27SB(S). This pre-rRNA is subsequently processed to the 5.8S(S) and 25S rRNAs. An alternative pathway leads to cleavage at site B1(L), the 5′ end of the 27SB(L) pre-rRNA, which is processed to yield the 5.8S(L) and 25S rRNAs. The B1(L)/5.8S(L) pathway does not require A3 *in cis* or RAT1p and XRN1p *in trans*, and is kinetically faster than the B1(S)/5.8S(S) pathway. In wild-type cells the ratio of the 5.8S(L) to 5.8S(S) rRNAs is ~1:8, presumably reflecting the relative utilization of the two pathways. Cleavage at B1(L) is drawn directly following cleavage at A2, but the mechanism of B1(L) formation is not known. Neither 27SA processing pathway has so far been shown to require snoRNP components, but the B1(S)/5.8S(S) pathway is likely to require RNase MRP. For simplicity, details of the processing of 27SB to 5.8S and 25S are not shown. It is not clear whether the 33S RNA is an intermediate in the major processing pathway, and the precise timing of the cleavage of the short 3′ ETS sequence is not known. (**C**) Structure of ITS1. The secondary structure predicted for ITS1 within the pre-rRNA is shown redrawn from Yeh *et al.* (1990). A number of nucleotides have been altered to match the sequence of the clone used for the pGAL::rDNA construct; none of these alter the predicted secondary structure. The mature 18S and 5.8S rRNA sequences are shaded. The 5′ end of ITS1 is numbered as nucleotide 1. The sites of A2, A3, B1(L) and B1(S) cleavage are indicated, as are the nucleotides modified to m_2^6A within the 18S rRNA. Large boxes enclose the nucleotides deleted in the ITS1Δ5′ and ITS1Δ3′ mutants. Nucleotides deleted in the A3Δ10 mutant are overlined; note that because of the sequence repeat in this region, this could also be drawn as a deletion of the 10 nucleotides flanking A3 to the 3′ side. The site indicated as A2 is that identified by primer extension and differs slightly from the site previously identified by S1 mapping (Veldman *et al.*, 1980).

1992) and the mitochondrial function of RNase MRP has been questioned. In yeast, mutations in the gene encoding the RNA component of RNase MRP (designated *NME1* or *RRP2*) (Schmitt and Clayton, 1992; Chu *et al.*, 1994) have been analyzed and shown to alter the ratio between the long and short forms of the 5.8S rRNA, which we term 5.8S(L) and 5.8S(S) respectively (Shuai and Warner, 1991; Lindahl *et al.*, 1992; Schmitt and Clayton, 1993). Mutations in the MRP RNA result in the under-accumulation of 5.8S(S) rRNA and the appearance of a low level of a 5′ extended version of the 5.8S rRNA which extends to site A2, but have little effect on the synthesis of 5.8S(L).

Mutation of another gene, *RAT1*, has also been reported to inhibit specifically the formation of the short form of yeast

5.8S rRNA (Amberg *et al.*, 1992). Mutations in *RAT1* were isolated as resulting in the nuclear accumulation of poly(A)$^+$ RNA, as judged by immunofluorescence (Amberg *et al.*, 1992). Other alleles of the same gene (designated *TAP1* and *HKE1*) have, however, been isolated using selection techniques which are not obviously related, although all potentially involve RNA metabolism (Aldrich *et al.*, 1993; Di Segni *et al.*, 1993; Kenna *et al.*, 1993). Another gene which plays a role in the metabolism of the pre-rRNA is *XRN1*. Mutations in *XRN1* lead to the accumulation of very high levels of the excised 5′ region of ITS1, between the 3′ end of the 18S rRNA and A2 (Stevens *et al.*, 1991) (see Figure 1). Again several different alleles of *XRN1* (designated *RAR5, KEM1, DST2* and *SEP1*) have been isolated using apparently unrelated selection techniques (reviewed by Kearsey and Kipling, 1991). Both the XRN1p and RAT1p proteins have 5′→3′ exonuclease activity *in vitro* (Stevens, 1980; Larimer *et al.*, 1992; Kenna *et al.*, 1993), suggesting that they might also function as exonucleases *in vivo*. Moreover, XRN1p and RAT1p have regions of substantial sequence homology (Kenna *et al.*, 1993), also suggesting that they might have related functions. It was therefore of interest to analyze the effects of single and double mutants of XRN1p and RAT1p on the processing of the pre-rRNA.

Although a considerable number of *trans*-acting factors required for yeast pre-rRNA processing have been identified, little is known about the role of *cis*-acting sequences in the pre-rRNA. A system for the functional analysis of pre-rRNA sequences, using neutral tags inserted into the 18S and 25S rRNA regions, has been reported (Musters *et al.*, 1989, 1990; van der Sande *et al.*, 1992) and we have previously made use of a variation of this technique to analyze the U3 binding site in the 5′ ETS (Beltrame and Tollervey, 1992). The range of biochemical techniques which can be used to analyze the mutants in this system is, however, rather limited. The production of the mature rRNAs can be measured and primer extension analysis can also be performed, but only using primers which hybridize to the tags in the 18S and 25S rRNA regions, which greatly limits their usefulness in the detailed analysis of the pre-rRNA processing pathway. We have therefore developed an alternative system for the analysis of mutations in the pre-rRNA. This makes use of strains in which the endogenous pre-rRNAs are conditionally expressed under the control of a thermosensitive (TS) RNA polymerase I (Wittekind *et al.*, 1988; Nogi *et al.*, 1993), in combination with the conditional expression of mutant pre-rRNAs under the control of an RNA polymerase II *GAL* promoter (Nogi *et al.*, 1991). This can be used to assess the effects of mutations in the pre-rRNA on growth and pre-rRNA processing. The use of this system for the detailed functional analysis of sequences in ITS1 is reported here. The analysis of one large deletion in the central region of ITS1 has previously been reported using a tagged rDNA construct (Musters *et al.*, 1990). This prevents the synthesis of 18S, but not 25S rRNA; detailed analysis of the processing of the mutant pre-rRNAs was, however, not possible.

From the analysis of the effects of *cis*- and *trans*-acting mutations we deduce a model for the formation of the 5′ end of the major form of 5.8S rRNA, involving endonucleolytic cleavage at a site designated A3, followed by exonuclease digestion.

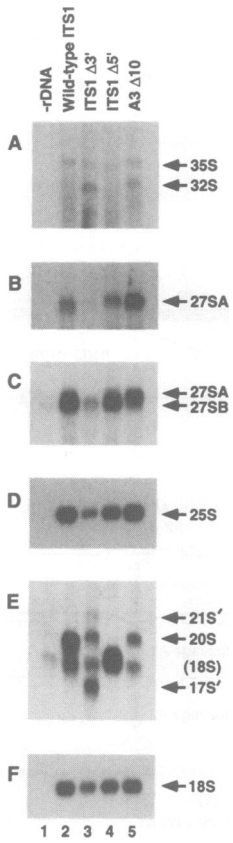

Fig. 2. Northern analysis of high molecular weight RNA from strains expressing mutant pre-rRNAs. Lane 1, RNA extracted from a strain carrying a plasmid lacking the rDNA sequence. Lane 2, RNA extracted from a strain carrying a plasmid with the rDNA containing the wild-type ITS1 sequence. Lane 3, RNA extracted from a strain carrying a plasmid with the rDNA containing the ITS1Δ3′ mutation. Lane 4, RNA extracted from a strain carrying a plasmid with the rDNA containing the ITS1Δ5′ mutation. Lane 5, RNA extracted from a strain carrying a plasmid with the rDNA containing the A3Δ10 mutation. (**A**) Hybridization with oligonucleotide g, which hybridizes in ITS2. (**B**) Hybridization with oligonucleotide d, which hybridizes in the 3′ region of ITS1. (**C**) Hybridization with oligonucleotide g, which hybridizes in ITS2. (**D**) Hybridization with oligonucleotide h, which hybridizes to the tag in the 25S rRNA. (**E**) Hybridization with oligonucleotide b, which hybridizes in the 5′ region of ITS1. (**F**) Hybridization with oligonucleotide a, which hybridizes to the tag in the 18S rRNA. For simplicity, we only show regions of each Northern; together these show all of the pre-rRNAs and rRNAs that we detect. Note that the gel mobilities of the 35S and 32S pre-rRNAs in the ITS1Δ3′ and ITS1Δ5′ strains, and the 20S pre-rRNA in the ITS1Δ5′ strain, are altered by the deletions in the pre-rRNA. The positions of the 35S, 32S, 27SA, 27SB and 20S pre-rRNAs, and the 25S and 18S rRNAs synthesized from pGAL::rDNA are indicated, as are two aberrant pre-rRNAs, 21S′ and 17S′, detected only in the ITS1Δ3′ mutant RNA. Oligonucleotide b cross-hybridizes with the 18S rRNA, which is indicated in brackets in panel E. RNA was extracted from *rpa12* strains carrying the plasmids indicated following growth for 6 h at 37°C, separated on a 1.2% agarose gel containing formaldehyde, and transferred for Northern hybridization.

Results

Development of a system for the functional analysis of sequences in the pre-rRNA

To test the effects of mutations in the pre-rRNA on ribosome synthesis we made use of plasmid pNOY102 (Nogi *et al.*, 1991) which has the entire pre-rRNA coding region placed between the *GAL7* promoter and terminator sequences. To

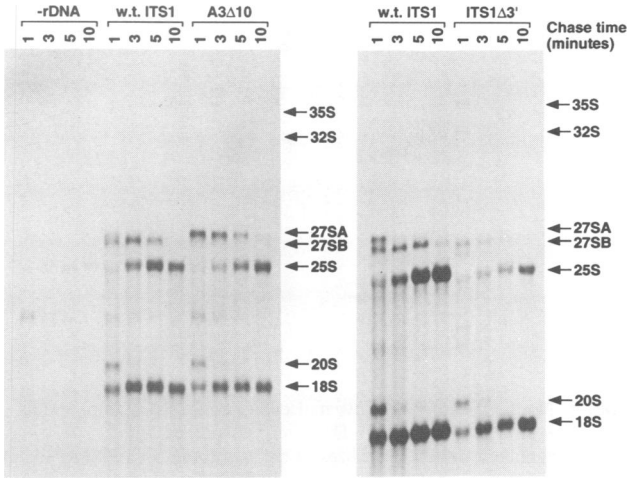

Fig. 3. Pulse−chase labeling of mutant pre-rRNAs. Labeling was performed using *rpa12* strains carrying a plasmid lacking the rDNA (−rDNA samples) or carrying pGAL::rDNA with the wild-type ITS1 sequence (wild-type ITS1 samples) or ITS1Δ3′ (ITS1Δ3′ samples) or A3Δ10 mutations (A3Δ10 samples). Following growth for 6 h at 37°C, cells were labeled with [^{3}H-methyl]methionine for 2 min, and then chased with a large excess of unlabeled methionine for the times indicated. RNA was separated on a 1.2% agarose gel containing formaldehyde and visualized by fluorography. The identity of the band intermediate in size between 25S and 18S, which is also seen in the −rDNA control samples, is unclear.

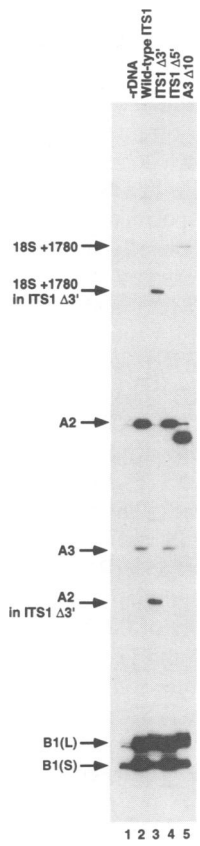

Fig. 4. Primer extension on ITS1 in mutant pre-rRNAs. Lane 1, RNA extracted from a strain carrying a plasmid lacking the rDNA sequence. Lane 2, RNA extracted from a strain carrying a plasmid with the rDNA containing the wild-type ITS1 sequence. Lane 3, RNA extracted from a strain carrying a plasmid with the rDNA containing the ITS1Δ3′ mutation. Lane 4, RNA extracted from a strain carrying a plasmid with the rDNA containing the ITS1Δ5′ mutation. Lane 5, RNA extracted from a strain carrying a plasmid with the rDNA containing the A3Δ10 mutation. The primer extension experiment shown was performed using oligonucleotide g, which hybridizes in ITS2. RNA was extracted from *rpa12* strains carrying the plasmids indicated following growth for 6 h at 37°C. The positions of primer extension stops due to cleavage of the pre-rRNA at sites A2, A3, B1(L) and B1(S) are indicated. The primer extension stops identified as 18S+1780 are due to the presence of two adjacent A residues (A1779 and A1780) in the 3′-most stem−loop structure of the 18S rRNA which are modified to m_2^6G (see Figure 1C) (Maden, 1990). These modifications occur on the 20S pre-rRNA in wild-type strains (Brand *et al.*, 1977) and can normally only be detected using an oligonucleotide which hybridizes to the pre-rRNA within the 20S pre-rRNA (data not shown). In the ITS1Δ3′ and A3Δ10 mutants, these modifications occur before cleavage at A2, i.e. on the 32S or 35S pre-rRNAs (see Figure 1B), due to the delay in A2 cleavage.

allow the identification of the mature rRNAs synthesized from the plasmid-borne rDNA, we inserted neutral tags in the 18S, 5.8S and 25S rRNA coding sequences into this plasmid (see Materials and methods), generating pGAL::rDNA. Plasmid pNOY102 has been shown to permit the growth of an *rpa135* strain, which lacks the 135 kDa subunit of RNA polymerase I (Nogi *et al.*, 1991). Since we expect that many mutations in the pre-rRNA will be lethal in this background, we wished to use a conditional mutation affecting RNA polymerase I. We initially used an *rpa190-1* strain, but in this strain growth at non-permissive temperature for long periods is required to deplete RNA polymerase I to low levels (Wittekind *et al.*, 1988); we found that growth of this strain for ≥24 h at 37°C was required for a 90% reduction in activity. After this extended period of growth at non-permissive temperature, the efficiency of pre-rRNA processing is impaired (data not shown). Subsequently, we found that in an *rpa12* mutant (Nogi *et al.*, 1993) the activity of RNA polymerase I is more rapidly lost; growth for 6 h at 37°C is sufficient for a 90% reduction in activity. Using the pGAL::rDNA plasmid in the *rpa12* strain, mutations in the pre-rRNA can be tested for their ability to support growth and their effects on pre-rRNA processing can be assessed by Northern hybridization, pulse−chase labeling and primer extension (see Figures 2−4). The kinetics of processing of the pre-rRNA synthesized from this plasmid are very similar to those of pre-rRNA transcribed from the chromosomal rDNA (Figure 3), and all tested cleavage sites are correct at the nucleotide level (Figure 4 and data not shown). There is a residual level of expression from the chromosomal rDNA which is seen in the '−rDNA' samples (which contain the same vector as pGAL::rDNA but lacking the rDNA coding region) in Figures 2−4. This is not high enough to interfere with the analysis of the mutations in the pre-rRNA. From the levels of the pre-rRNAs detected by Northern hybridization and the total incorporation in pulse labeling experiments, we estimate that pre-rRNA transcription in *rpa12* strains complemented by pGAL::rDNA is ~30% of that in wild-type cells.

Analysis of the effects of large deletions in ITS1

We wished to use this system for the detailed analysis of the effects of mutations in ITS1. As an initial experiment, large deletions of most of the 5′ region (ITS1Δ5′, see Figure 1C) or 3′ region of ITS1 (ITS1Δ3′, see Figure 1C) were constructed on either side of A2, the only cleavage site then known in ITS1. The end points were chosen so as not to affect the predicted secondary structures around A2 and

B1. These mutations were tested in the pGAL::rDNA construct. Somewhat surprisingly, both constructs support growth of the strain at non-permissive temperature, although *rpa12* strains complemented by the ITS1Δ3′ construct have a reduced growth rate. Strains complemented by the wild-type pGAL::rDNA have a doubling time of 6.5 h in galactose minimal medium, while ITS1Δ3′ strains have a doubling time of 12 h at the non-permissive temperature. The results of detailed analyses of the effects of mutations around sites A2 and B1 will be presented elsewhere.

The effects of the ITS1Δ5′ and ITS1Δ3′ mutations on the processing of pre-rRNA were assessed by Northern hybridization and pulse–chase labeling (see Figure 1B for an outline of the pre-rRNA processing pathway). The ITS1Δ5′ mutation has little effect on the steady-state levels of the large rRNAs or pre-rRNAs. Hybridization with probes against the tags in the 25S (Figure 2D) and 18S (Figure 2F) rRNAs shows that the ITS1Δ3′ mutation reduces the synthesis of both the 25S and 18S rRNAs, with a stronger effect on the synthesis of 25S rRNA. The ITS1Δ3′ mutation leads to a mild accumulation of the 32S pre-rRNA (Figure 2A; the mobility of the 35S and 32S pre-rRNAs is altered in the ITS1Δ3′ and ITS1Δ5′ strains because of the large deletions) indicating some delay in processing at site A2. The levels of both 27SA and 27SB are reduced in the ITS1Δ3′ mutant (Figure 2B and C; 27SA and 27SB are not resolved in the ITS1Δ3′ strain because of the deletion). The steady-state level of 20S pre-rRNA is not affected by the ITS1Δ5′ mutation (Figure 2E; the mobility of 20S is altered by the deletion in ITS1Δ5′) but is reduced in the ITS1Δ3′ strain (Figure 2E). Two additional aberrant pre-rRNAs are detected in the ITS1Δ3′ strain; these are designated 21S′ and 17S′ in Figure 2E. These RNAs also hybridize to oligonucleotide d, which lies at the 3′ end of ITS1, but do not hybridize to oligonucleotide g (data not shown), which lies in ITS2. From its size and hybridization pattern, the 21S′ pre-rRNA may run from the 5′ end of the 18S rRNA to the 3′ end of 5.8S, and would be synthesized by processing of ITS2 in the absence of processing in ITS1. Surprisingly, the 5′ end of the 17S′ RNA must lie within the 18S coding region. Only strains mutated in the RNA component of RNase MRP have previously been found to synthesize a pre-rRNA species cleaved within the mature 18S rRNA region (Shuai and Warner, 1991). Oligonucleotide b cross-hybridizes with the 18S rRNA, which is visible in all lanes in Figure 2E.

The effects of the mutations in ITS1 on the processing of the pre-rRNA were also assessed by pulse–chase labeling (Figure 3). In strains carrying the ITS1Δ3′ mutation the synthesis of 18S rRNA is reduced but the synthesis of 25S rRNA is more strongly inhibited. Processing of the 35S and 32S pre-rRNAs is very rapid in wild-type strains, and even at the shortest chase times, most has been processed to 27SA and 20S pre-rRNA. In the ITS1Δ3′ mutant, 35S and 32S pre-rRNA are processed more slowly and are still visible at the earliest chase time point. The 27SA and 27SB pre-rRNAs are not resolved in the ITS1Δ3′ mutant, but an additional pre-rRNA species smaller than 27SB is reproducibly seen in labeling of the ITS1Δ3′ strain; this does not obviously correspond to an RNA detected by Northern hybridization and its identity is not clear at present. Pulse–chase labeling of the strain carrying the ITS1Δ5′ mutation did not reveal any clear differences in the processing pathway (data not shown), consistent with the results of Northern hybridization.

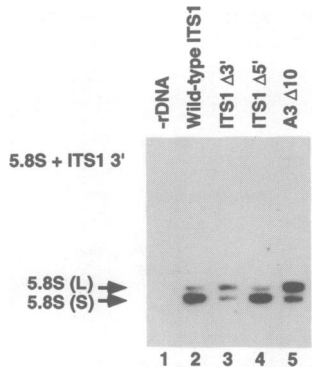

Fig. 5. Northern analysis of low molecular weight RNA from strains expressing mutant pre-rRNAs. The filter was probed with oligonucleotide f, which hybridizes to the tag in the 5.8S rRNA. Lane 1, RNA extracted from a strain carrying a plasmid lacking the rDNA sequence. Lane 2, RNA extracted from a strain carrying a plasmid with the rDNA containing the wild-type ITS1 sequence. Lane 3, RNA extracted from a strain carrying a plasmid with the rDNA containing the ITS1Δ3′ mutation. Lane 4, RNA extracted from a strain carrying a plasmid with the rDNA containing the ITS1Δ5′ mutation. Lane 5, RNA extracted from a strain carrying a plasmid with the rDNA containing the A3Δ10 mutation. RNA was extracted from *rpa12* strains carrying the plasmids indicated following growth for 6 h at 37°C, separated on an 8% polyacrylamide gel containing 8.3 M urea and transferred for Northern hybridization.

Primer extension was used to analyze the effects of the mutations in ITS1 on cleavage at A2, B1 and other processing sites in more detail. None of the mutations alter the accuracy of cleavage at the 5′ end of the 18S rRNA at site A1 or at the 5′ end of 25S rRNA at site C1, nor do they affect the accuracy or efficiency of cleavage in the 5′ ETS at site A0 (see Figure 1A and B) (data not shown). Processing within ITS1 was analyzed by primer extension using primers d, e, g and h (see Figure 1A) (shown for primer g in Figure 4; primer extension with oligonucleotide h, which hybridizes within the mature 25S rRNA gave very similar results). The level of the primer extension products which terminate at site A2 reflects the abundance of the 27SA pre-rRNA (see Figure 1B). Primer extension on RNA from the ITS1Δ5′ strain (Figure 4, lane 4), shows that this mutation does not affect the abundance of 27SA pre-rRNA or the accuracy of cleavage at site A2. The ITS1Δ3′ mutation (Figure 4, lane 3) reduces the level of the 27SA pre-rRNA ~5-fold, but does not affect the accuracy of processing at site A2.

The pre-rRNA processing site previously referred to as B1, is in fact comprised of two major sites which we designate B1(L) and B1(S) (see Figure 1B and C). The primer extension stops at B1(L) and B1(S) correspond to the 5′ ends of the two forms of the 27SB pre-rRNA, designated 27SB(L) and 27SB(S) respectively (see Figure 1B). The ITS1Δ5′ mutation does not alter the abundance of 27SB(L) or 27SB(S) (Figure 4, lane 4). In the ITS1Δ3′ strain, the level of 27SB(S) is reduced to a level close to that of the residual chromosomal rDNA expression [Figure 4, compare levels of B1(S) in lanes 1 and 3], showing that little of the ITS1Δ3′ pre-rRNA is processed to 27SB(S). In contrast, the level of 27SB(L) pre-rRNA is unchanged in the ITS1Δ3′ mutant.

Sites B1(L) and B1(S), the 5′ ends of the 27SB(L) and

27SB(S) pre-rRNAs, also correspond to the 5′ ends of the mature 5.8S(L) and 5.8S(S) rRNAs respectively (see Figure 1B). This shows that the mature 5.8S(L) and 5.8S(S) rRNAs cannot themselves have a precursor/product relationship. Selective inhibition of the formation of the 27SB(S) pre-rRNA should therefore inhibit the synthesis of the 5.8S(S), but not the 5.8S(L) rRNA. To test this, we hybridized a Northern transfer of RNA from the ITS1 mutant strains (Figure 5) using a probe specific for the tag in the 5.8S rRNA (oligonucleotide f in Figure 1A). The ITS1Δ3′ mutation strongly reduces the synthesis of 5.8S(S), resulting in reduced overall synthesis of 5.8S rRNA. As expected, the reduction in 5.8S rRNA synthesis is similar to the reduction in the synthesis of 25S rRNA.

In conclusion, the deletion of most of the 5′ region of ITS1 has, surprisingly, little effect on the accuracy or efficiency of pre-rRNA processing. Deletion of the 3′ region of ITS1 inhibits cleavage at site A2. Probably as a consequence of this, synthesis of 27SA pre-rRNA is reduced, resulting in the under-accumulation of both the 5.8S and 25S rRNAs. The most striking effect of this deletion is, however, its selective inhibition of synthesis of 27SB(S) relative to 27SB(L). We conclude that a site in the 3′ region of ITS1 is required *in cis* for the formation of the 5′ end of the 27SB pre-rRNA at site B1(S) but not B1(L), and in consequence is required for the synthesis of 5.8S(S) but not 5.8S(L) rRNA.

Identification of A3, a novel cleavage site in ITS1 required in cis for 5.8S(S) formation

Previous results from Northern hybridization and pulse–chase labeling have led us to conclude that the genetic depletion of a number of different components of the snoRNPs leads to the inhibition of cleavage at sites A1 and A2 (Li *et al.*, 1990; Hughes and Ares, 1991; Tollervey *et al.*, 1991; Girard *et al.*, 1992; Jansen *et al.*, 1993; Morrissey and Tollervey, 1993). To confirm this model, we performed primer extension through site A2 in ITS1 using primers in ITS1, in the 5.8S coding region and in ITS2 (oligonucleotides d, e and g in Figure 1A). All of these analyses showed that depletion of the snoRNAs U3, U14 or snR30, or the snoRNP proteins, NOP1p, GAR1p or SOF1p, does indeed lead to reduction in cleavage at site A2 (shown for snR30, NOP1 and GAR1 in Figure 6). All of these components are expressed under the control of inducible *GAL* promoters; the different components are depleted at different rates following transfer of the strains to glucose medium, and this is reflected in the different depletion time courses used. Under repressing conditions, such promoters are not completely inactive, and the low level of residual synthesis of the snoRNP components may be responsible for the residual A2 cleavage. During the course of these analyses, we observed that in addition to reducing cleavage at site A2, depletion of snR30 leads to an increase in primer extension arrest at a site which we designated A3 (Figure 6). This effect was not seen on depletion of U3, U14, NOP1p, GAR1p or SOF1p (shown for NOP1p and GAR1p in Figure 6). Moreover, the primer extension stop at A3 is not lost on depletion of any of these components. No primer extension stop at A3 is detected in pre-rRNA transcribed *in vitro* (see below), making it unlikely that it is due to an effect of the secondary structure. Strains carrying *GAL::snr30* are mildly impaired in the processing of pre-rRNA even during growth on galactose medium, probably because the level of snR30 which is synthesized in the *GAL::snr30* strains is lower than in *SNR30* strains and is heterogeneous at its 5′ end (Morrissey and Tollervey, 1993). The level of the primer extension stop at A3 is also elevated during growth of the *GAL::snr30* strain on galactose medium (Figure 6, lane 2). The A3 cleavage site can also be detected by primer extension using an oligonucleotide within the 25S rRNA region (oligonucleotide h in Figure 1A) (data not shown), demonstrating that this cleavage forms the 5′ end of an RNA species including the 3′ region of ITS1, the 5.8S

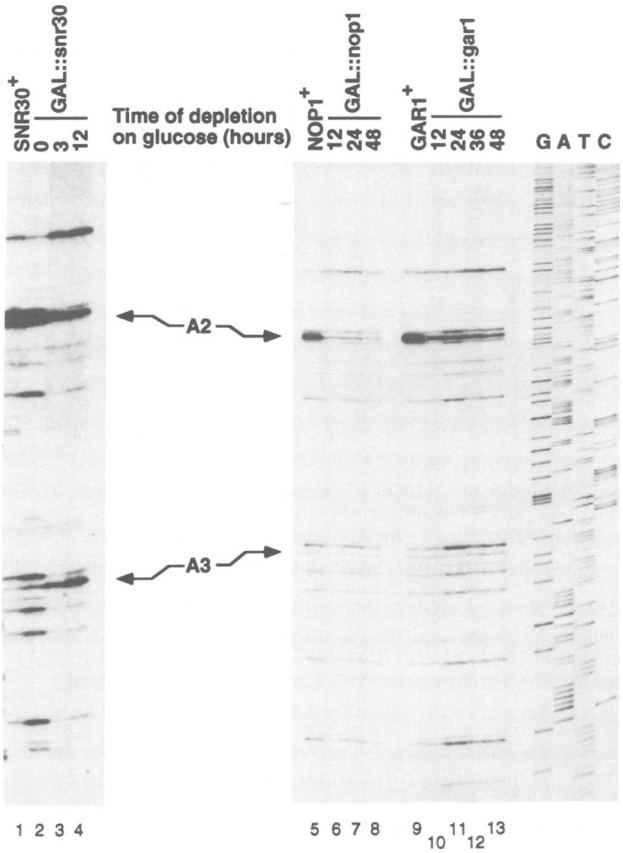

Fig. 6. Primer extension on ITS1 using RNA from strains depleted of snoRNP components. Primer extension was performed using oligonucleotide e, which hybridizes within the 5.8S rRNA. Lane 1, RNA extracted from a strain with the wild-type *SNR30* gene following growth on glucose medium for 12 h. Lane 2, RNA extracted from a *GAL::snr30* strain following growth on galactose medium. Lane 3, RNA extracted from a *GAL::snr30* strain following growth on glucose medium for 3 h. Lane 4, RNA extracted from a *GAL::snr30* strain following growth on glucose medium for 12 h. Lane 5, RNA extracted from a strain with the wild-type *NOP1* gene following growth on glucose medium for 24 h. Lane 6, RNA extracted from a *GAL::nop1* strain following growth on glucose medium for 12 h. Lane 7, RNA extracted from a *GAL::nop1* strain following growth on glucose medium for 24 h. Lane 8, RNA extracted from a *GAL::nop1* strain following growth on glucose medium for 48 h. Lane 9, RNA extracted from a strain with the wild-type *GAR1* gene following growth on glucose medium for 24 h. Lane 10, RNA extracted from a *GAL::gar1* strain following growth on glucose medium for 12 h. Lane 11, RNA extracted from a *GAL::gar1* strain following growth on glucose medium for 24 h. Lane 12, RNA extracted from a *GAL::gar1* strain following growth on glucose medium for 36 h. Lane 13, RNA extracted from a *GAL::gar1* strain following growth on glucose medium for 48 h. The positions of primer extension stops due to cleavage of the pre-rRNA at sites A2 and A3 are indicated. DNA sequencing reactions using oligonucleotide e are also shown.

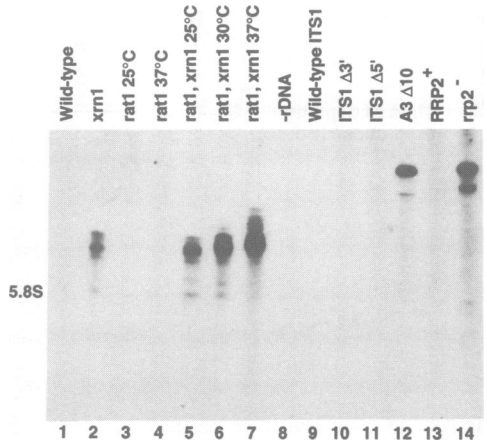

Fig. 7. Northern analysis of 5′ extended forms of 5.8S rRNA. The filter was probed with oligonucleotide d, which hybridizes to the 3′ region of ITS1. Lane 1, RNA extracted from an *XRN1* strain of yeast. Lane 2, RNA extracted from an otherwise isogenic *xrn1::URA3* strain. Lane 3, RNA extracted from a *rat1-1* strain following growth at 25°C. Lane 4, RNA extracted from a *rat1-1* strain following growth at 37°C. Lane 5, RNA extracted from a *rat1-1*; *xrn1::URA3* strain following growth at 25°C. Lane 6, RNA extracted from a *rat1-1*; *xrn1::URA3* strain following growth at 30°C. Lane 7, RNA extracted from a *rat1-1*; *xrn1::URA3* strain following growth at 37°C. Lane 8, RNA extracted from an *rpa12* strain carrying the pGAL::rDNA vector lacking the rDNA sequence. Lane 9, RNA extracted from an *rpa12* strain carrying pGAL::rDNA containing the wild-type ITS1 sequence. Lane 10, RNA extracted from an *rpa12* strain carrying pGAL::rDNA containing the ITS1Δ3′ mutation. Lane 11, RNA extracted from an *rpa12* strain carrying pGAL::rDNA containing the ITS1Δ5′ mutation. Lane 12, RNA extracted from an *rpa12* strain carrying pGAL::rDNA containing the A3Δ10 mutation. Lane 13, RNA extracted from a wild-type strain. Lane 14, RNA extracted from an *rrp2* strain. RNA was extracted from the wild-type and *xrn1* strains following growth at 30°C, from the *RRP2* and *rrp2* strains following growth at 25°C, from the *rat1* and *rat1*; *xrn1* strains following growth for 2 h at the temperature indicated, and from *rpa12* strains carrying the plasmids indicated following growth for 6 h at 37°C. RNA was separated on an 8% polyacrylamide gel containing 8.3 M urea and transferred for Northern hybridization. The gel mobility of 5.8S rRNA is indicated for comparison.

coding region, ITS2 and the 25S rRNA coding region (see Figure 1B). We designate this pre-rRNA species 27SA′. The 27SA′ pre-rRNA is not readily detected by pulse−chase labeling, probably because it has a very short life time and is not clearly resolved from the 27SA and 27SB pre-rRNAs. A band of the predicted mobility can, however, be observed following very long migration of the gels (data not shown). We conclude that A3 is a previously unidentified processing site, which continues to be cleaved in the absence of several different snoRNP components.

Since A3 is located in the 3′ region of ITS1, it was a candidate to be the site required *in cis* for processing at B1(S). To test this we constructed a deletion of 10 nucleotides surrounding site A3 (A3Δ10) (see Figure 1C). The A3Δ10 mutation supports wild-type growth, and its effects on pre-rRNA processing were assessed as described above for the large ITS1 deletions. Hybridization with probes against the tags in the 25S (Figure 2D) and 18S rRNAs (Figure 2F) shows little effect on the steady-state levels of the large rRNAs. No accumulation of the 35S primary transcript is detected but there is a mild accumulation of the 32S pre-rRNA (Figure 2A) indicating some delay in processing at site A2. The steady-state level of 20S pre-rRNA is also reduced in the A3Δ10 strain (Figure 2E). The A3Δ10 mutation leads to a strong accumulation of the 27SA pre-rRNA (Figure 2B) and a concomitant reduction in the level of 27SB (Figure 2C), indicating that processing subsequent to A2 cleavage is strongly delayed. In pulse−chase labeling (Figure 3), the A3Δ10 mutation does not impair synthesis of the 25S or 18S rRNAs but strongly delays the processing of 27SA, and also results in some delay in the synthesis of 25S rRNA. On longer exposures, a low level of the 27SB pre-rRNA is detected in the A3Δ10 strain (data not shown). These results are in good agreement with the results of Northern hybridization. Primer extension shows that, as expected, the A3Δ10 mutation results in the loss of the primer extension stop at A3 (Figure 4, lane 5), although on long exposures a low level of residual cleavage can be detected. As shown by the alteration in the primer extension stops at sites B1(S) and B1(L), synthesis of 27SB(S) from the A3Δ10 pre-rRNA is strongly reduced, while the steady-state level of 27SB(L) is either unchanged or mildly reduced in different experiments. B1(L) is itself heterogeneous, with two major stops; in the pre-rRNA from A3Δ10 strain, the position of the major B1(L) primer extension stops is shifted one or two nucleotides 5′.

Hybridization of the Northern transfer of low molecular weight RNA (Figure 5) shows that the A3Δ10 mutation reduces 5.8S(S) formation but increases the synthesis of 5.8S(L), so that overall synthesis of 5.8S rRNA is unchanged. In the wild-type and ITS1Δ5′ strains the ratio of 5.8S(L):(S) is ~1:8. This is altered to ~8:1 in the A3Δ10 strain. The accumulation of the 5.8S(L) rRNA in the A3Δ10 mutants also confirms that the mature 5.8S(L) and 5.8S(S) rRNAs do not have a precursor/product relationship.

In addition, the A3Δ10 mutation results in the accumulation of a low level of an extended form of 5.8S rRNA (faintly visible at the exposure shown in Figure 5, lane 5). Hybridization with probes specific for ITS1 and 2 (probes c, d and g in Figure 1A) shows that this RNA extends into ITS1 (Figure 7, lane 12). The gel mobility of this 5′ extended form of 5.8S is consistent with its extending from the 3′ end of 5.8S to site A2. This RNA is hybridized by oligonucleotide c, the 3′ end of which lies exactly at the A2 cleavage site. When allowance is made for the 10 nucleotide deletion carried by the A3Δ10 RNA, this band co-migrates with the form of 5.8S extended to site A2 seen in *rrp2* strains, which are mutant for the RNA component of RNase MRP (Shuai and Warner, 1991; Lindahl *et al.*, 1992; Chu *et al.*, 1994; Schmitt and Clayton, 1993) (Figure 7, compare lanes 12 and 14). This suggests that, like mutations in RNase MRP, the A3Δ10 mutation may result in the accumulation of a low level of a form of 5.8S rRNA which is 3′ mature but extends to site A2. On longer exposures, a larger RNA species is detected by hybridization with probes c, d and g; the size and hybridization pattern of this RNA are consistent with its extending from A2 to C2 (see Figure 1A) (data not shown). This would arise if processing in ITS2 occurred prior to processing at B1 in the A3Δ10 mutant pre-rRNA.

In conclusion, we have shown that site A3 is required *in cis* for the formation of the 5′ end of 27SB(S) pre-rRNA at site B1(S), and therefore for the synthesis of 5.8S(S). In the absence of A3, processing of 27SA pre-rRNA is strongly delayed, and processing is transferred predominantly to site B1(L), generating 27SB(L) and 5.8S(L). The delay in processing at B1 may be due to the inability of the B1(L)

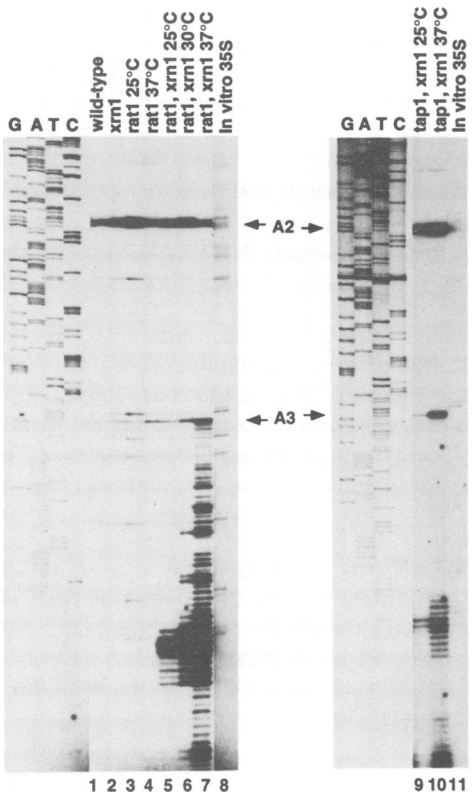

Fig. 8. Primer extension on ITS1 using RNA from strains mutant for *RAT1* and *XRN1*. Primer extension was performed with oligonucleotide e, which hybridizes within the 5.8S rRNA. Lane 1, RNA extracted from an *XRN1* strain. Lane 2, RNA extracted from an otherwise isogenic *xrn1::URA3* strain. Lane 3, RNA extracted from a *rat1-1* strain following growth at 25°C. Lane 4, RNA extracted from a *rat1-1* strain following growth at 37°C. Lane 5, RNA extracted from a *rat1-1*; *xrn1::URA3* strain following growth at 25°C. Lane 6, RNA extracted from a *rat1-1; xrn1::URA3* strain following growth at 30°C. Lane 7, RNA extracted from a *rat1-1*; *xrn1::URA3* strain following growth at 37°C. Lane 8, RNA transcribed *in vitro* from a plasmid expressing the full-length 35S pre-rRNA under the control of a T3 promoter. Lane 9, RNA extracted from a *tap1-1; xrn1::URA3* strain following growth at 25°C. Lane 10, RNA extracted from a *tap1-1; xrn1::URA3* strain following growth at 37°C. Lane 11, RNA transcribed *in vitro* from a plasmid expressing the full-length 35S pre-rRNA under the control of a T3 promoter. RNA was extracted from the wild-type and *xrn1* strains following growth at 30°C, and from the *rat1*, *rat1*; *xrn1* and *tap1*; *xrn1* strains following growth for 2 h at the temperature indicated. DNA sequencing reactions using oligonucleotide e are also shown.

processing system to cope with the increased flux. Because of this delay, processing within ITS2 also occurs directly on the 27SA pre-rRNA in the A3Δ10 strain.

The role of exonucleases in the formation of 5.8S rRNA

Two yeast proteins, RAT1p and XRN1p, have been reported to have 5′→3′ exonuclease activity *in vitro* (Stevens, 1980; Larimer *et al.*, 1992; Kenna *et al.*, 1993), and to have effects on pre-rRNA processing *in vivo* (Stevens *et al.*, 1991; Amberg *et al.*, 1992). 5′ extended forms of 5.8S rRNA are detected in strains carrying mutations in the *RAT1* and *XRN1* genes, but these are shorter than the RNAs seen in A3Δ10 strains (Figure 7, compare lanes 5–7 with lane 12). A low level of the 5′ extended 5.8S rRNA species is detected in *xrn1::URA3* single mutant strains (Figure 7, lane 2), but this is greatly increased in *rat1-1*; *xrn1::URA3* double mutant strains, particularly following growth for 2 h at 37°C, the non-permissive temperature for the *rat1-1* mutation (Figure 7, lane 7). We also analyzed strains carrying the *tap1-1* mutation, which is allelic with *RAT1*. Strains carrying the *tap1-1*; *xrn1::URA3* mutations accumulate the 5′ extended form of 5.8S rRNA seen in *rat1-1*; *xrn1::URA3* strains (data not shown). Northern hybridization with other pre-rRNA probes indicates that the accumulation of a number of excised fragments of the pre-rRNA spacers is greatly increased in the double mutant strains. These include fragments with sizes and hybridization patterns appropriate for the excised A0–A1 and A2–A3 regions (see Figure 1A) (data not shown), indicating that these are all sites of endonucleolytic cleavage. Northern hybridization for high molecular weight pre-rRNAs did not show any clear differences between wild-type and *rat1-1*; *xrn1::URA3* strains (data not shown).

Primer extension was used to identify the 5′ ends of the extended forms of 5.8S rRNA in *rat1-1*; *xrn1::URA3* and *tap1-1*; *xrn1::URA3* strains (Figure 8). This reveals a strong ladder of RNA species which extend from the 5′ end of 5.8S to site A3, but not beyond. The level of RNA species which extend to A3 is mildly increased in *xrn1::URA3* strains and in *rat1-1* strains following growth for 2 h at 37°C (Figure 8, lanes 2 and 4). This is increased in *rat1-1*; *xrn1::URA3* double mutant strains, particularly following growth at 37°C (Figure 8, lane 7). Strains carrying the *tap1-1*; *xrn1::URA3* mutations also accumulate the ladder of pre-rRNAs but have a higher level of RNA species which extend to A3 (Figure 8, lane 10) as compared with the *rat1-1*; *xrn1::URA3* strain. We conclude that 5′→3′ exonuclease activity, which requires RAT1p and XRN1p, digests from site A3 to B1. The strong stops 3′ of A3 seen in the mutants even at permissive temperature, correspond to the position of the base of the 5′ side of the stem structure which includes the B1 sites (centered on nucleotides A_{332} and G_{333}; see Figure 1C), suggesting that the residual exonuclease activity in the double mutant strains can digest single-stranded regions of the pre-rRNA more readily than double-stranded regions. Note that primer extension stops at sites A2 and A3 are not detected in RNA transcribed *in vitro* from the full-length rDNA under the control of a T3 RNA polymerase promoter (Figure 8, lanes 8 and 11), showing that these stops are not due to secondary structure in the pre-rRNA. In addition, in *rat1-1* or *tap1-1* single mutant strains, the positions of the major B1(L) primer extension stops are displaced one or two nucleotides 5′, as is the case for A3Δ10 strains (see above) (data not shown). This cannot readily be assessed in the double mutant strains because of the ladder of bands extending 5′ from B1.

The effects of mutations in *RAT1* and *XRN1* on the synthesis of 5.8S rRNA was further investigated by pulse–chase labeling of low molecular weight RNA with [^{3}H]uracil. No clear effects on the kinetics or efficiency of synthesis of 5.8S(S) or 5.8S(L) rRNA were seen on pulse–chase labeling of *xrn1::URA3* single mutant strains (data not shown). The effects of the *rat1-1*; *xrn1::URA3* double mutations were assessed following growth for 1.5 h at 37°C, the non-permissive temperature for *rat1-1* (Figure 9). Equivalent exposures are shown for the wild-type and mutant strains; the mutant clearly has a reduced level of incorporation into all small RNA species, possibly

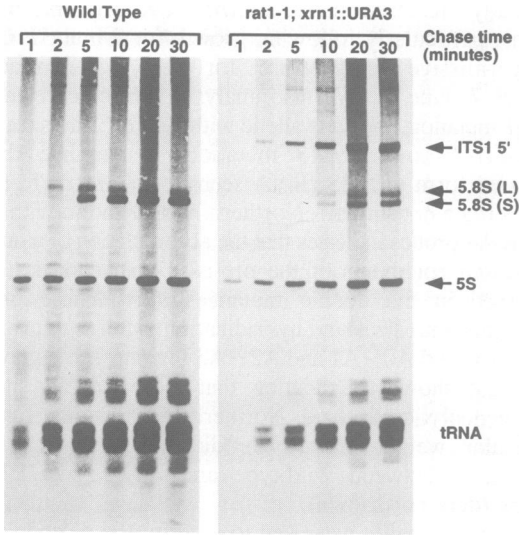

Fig. 9. Pulse–chase labeling of low molecular weight RNA in *rat1-1*; *xrn1::URA3* and wild-type strains. Cells grown for 1.5 h at 37°C were pulse-labeled for 1 min with [^{3}H]uracil and then chased with a large excess of unlabeled uracil for the times indicated. The positions of the 5.8S(L), 5.8S(S) and 5S rRNAs and tRNA are indicated, as is the band corresponding to the 5′ region of ITS1 which accumulates in the *rat1-1*; *xrn1::URA3* strain.

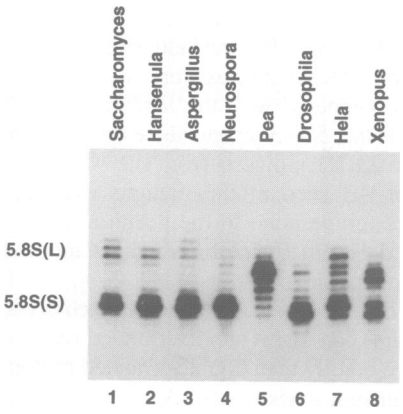

Fig. 10. Primer extension through the 5′ end of 5.8S rRNA in a range of eukaryotes. Primer extension was performed using oligonucleotide e, which hybridizes within the 5′ region of the 5.8S rRNA. RNA was extracted from *Saccharomyces cerevisiae* (lane 1), *Hansenula wingei* (lane 2), *Aspergillus nidulans* (lane 3), *Neurospora crassa* (lane 4), *Pisum sativum* (lane 5), *Drosophila melanogaster* (lane 6), HeLa cells (lane 7) and *Xenopus laevis* oocytes (lane 8). The positions of the 5.8S(L) and 5.8S(S) rRNAs from *S.cerevisiae* are indicated.

simply as a consequence of its impaired growth at the non-permissive temperature. Synthesis of 5.8S(S) rRNA is, however, inhibited more than the synthesis of 5.8S(L), 5S rRNA or tRNA. As judged by pulse–chase labeling or ethidium bromide staining of total RNA (data not shown), the level of 5.8S(L) rRNA as a fraction of total RNA is greater in *rat1-1*; *xrn1::URA3* strains than in the wild-type. However, the synthesis of both the 5.8S(L) and 5.8S(S) rRNAs is kinetically delayed in the mutant. The reason for this is not clear at present. The prominent band above 5.8S rRNA is the 5′ region of ITS1 which strongly accumulates in *xrn1* mutant strains independent of mutations in *RAT1* (Stevens *et al.*, 1991). It is notable that in the wild-type strain 5.8S(L) rRNA appears before 5.8S(S) rRNA. As discussed above, the mature 5.8S(L) and 5.8S(S) rRNAs cannot have a precursor/product relationship. 5.8S(L) rRNA must therefore be generated by a kinetically faster pathway than 5.8S(S) rRNA.

5′ end heterogeneity in 5.8S rRNA from other eukaryotes

Since the 5′ end heterogeneity of yeast 5.8S rRNA appears to be due to the use of two distinct processing pathways, we were interested to see the extent to which this heterogeneity is found in other eukaryotes. We therefore prepared RNA from a distantly related budding yeast, *Hansenula wingei*, two filamentous fungi, *Aspergillus nidulans* and *Neurospora crassa*, a higher plant, *Pisum sativum* (pea), an insect, *Drosophila melanogaster*, and cells from two vertebrates, HeLa cells (human) and *Xenopus laevis* oocytes. These were analyzed by primer extension from within the 5.8S rRNA coding region, using oligonucleotides to phylogenetically conserved sequences (Figure 10). In every case the 5′ end of 5.8S rRNA is heterogeneous, although the ratio between the 5.8S(L) and 5.8S(S) rRNAs varies, with pea having 5.8S(L) as the major species, and *Xenopus* having equal amounts of the 5.8S(L) and 5.8S(S) rRNAs.

Discussion

One of the major problems slowing the analysis of eukaryotic ribosome synthesis has been the lack of tractable systems for the functional analysis of signals in the pre-rRNA and rRNA. *In vitro* systems which generate the mature rRNAs have not so far been reported, and genetic analyses have been hampered by the fact that the rDNA is present in ~150 copies and is, moreover, essential for viability. We circumvent these problems by the use of a conditional mutation affecting RNA polymerase I (Nogi *et al.*, 1993), in combination with a plasmid, pGAL::rDNA, which expresses the rDNA under the control of an RNA polymerase II, *GAL* promoter. It has previously been shown that a variant of this construct will support growth in strains deleted for a subunit of RNA polymerase I (Nogi *et al.*, 1991); here we show that in an *rpa12* mutant strain grown at non-permissive temperature on galactose medium, the pGAL::rDNA plasmid provides >90% of ribosomal RNA transcription. The kinetics of processing of pre-rRNA molecules transcribed from the plasmid are identical to those transcribed from the chromosomal rDNA and all known processing sites are correct to the nucleotide. With this system, we are now in a position to analyze, at the nucleotide level, the sites and signals required *in cis* for pre-rRNA processing. Mutations can be analyzed using all of the techniques that have previously been applied to the study of the effects of *trans*-acting components, i.e. pulse–chase labeling, Northern hybridization with probes specific for the pre-rRNAs and primer extension. Moreover, mutations in either the pre-rRNA or the mature rRNA can be rapidly tested for their ability to support growth. This system should also allow the detailed analysis of the effects of mutations in the mature rRNA domains on ribosome assembly and function.

To test the requirements for *cis*-acting sequences in ITS1, we constructed deletions of most of the 5′ region (ITS1Δ5′)

or 3′ region of ITS1 (ITS1Δ3′). Somewhat surprisingly, both mutations support growth, although the ITS1Δ3′ mutant strains have an increased doubling time. This mutation results in reduced cleavage at A2 and, consistent with this, reduces synthesis of the 20S and 27SA pre-rRNAs (see Figure 1B). It is not clear whether the reduction in A2 cleavage is due to the deletion of specific signals in pre-rRNA, or is due to perturbation of the secondary structure. The processing site previously referred to as B1, in fact consists of two major sites which we designate B1(L) and B1(S). The ITS1Δ3′ mutation selectively inhibits processing at B1(S) reducing the synthesis of 27SB(S) pre-rRNA and 5.8S(S) rRNA (see Figure 1B). This indicates that a site in the 3′ region of ITS1 is important for processing at B1(S), but not B1(L). In contrast, the deletion of most of the 5′ region of ITS1 has little effect on pre-rRNA processing.

Depletion of the snoRNA, snR30, results in increased cleavage at a previously unidentified site, designated A3, which lies in the 3′ region of ITS1. This effect is specific for snR30 and is not seen on depletion of other snoRNAs (U3, U14, snR10) or snoRNP proteins (NOP1, GAR1 and SOF1); depletion of any of these reduces the efficiency of cleavage at A2, but does not affect the specificity. Comparison of the primary sequences of sites A2 and A3 shows that the four nucleotides 3′ to the cleavage site are identical (see Figure 1C). 3′ to this region of conservation, the sequence flanking A2 has the potential to form seven consecutive base-pairs with the 5′ end of snR30 (data not shown), but no such complementarity can be found for A3. The functional significance of this potential interaction is currently being tested. It is possible that an interaction between snR30 and site A2 constrains the processing machinery to cleave site A2 before A3; in the absence of this interaction cleavage at A3 may be able to occur earlier than in wild-type cells, resulting in an increase in the steady-state level of A3 cleaved pre-rRNAs. When the early cleavages at sites A0, A1 and A2 (see Figure 1B) are inhibited by depletion of the snoRNAs or the snoRNP proteins, an aberrant 23S pre-rRNA is detected which has a 3′ end in the 3′ region of ITS1 between sites A2 and B1. This is presumably due to the presence of a cleavage site in this region which continues to be used in strains depleted for the snoRNPs. Since site A3 continues to be cleaved in the depleted strains, it is very likely that this site forms the 3′ end of the 23S pre-rRNAs in these mutants.

To test the requirement for A3 *in cis*, we constructed a 10 nucleotide deletion at this site (A3Δ10). This strongly inhibits processing at B1(S) and the synthesis of the 27SB(S) pre-rRNA and 5.8S(S) rRNA (see Figure 1B). With the A3Δ10 mutation *in cis*, most processing is transferred to the alternative B1(L)/5.8S(L) pathway, and the 5.8S(L):5.8S(S) rRNA ratio changes from ~1:8 in wild-type strains to ~8:1 in the mutant. The A3Δ10 mutation does not prevent processing at site A2 but causes a mild delay in cleavage. Despite this, the 27SA pre-rRNA, which is generated by A2 cleavage, accumulates in the A3Δ10 strain because the subsequent processing steps are more strongly delayed. The delay in A2 cleavage may be due to depletion of the processing machinery by binding to the accumulated 27SA pre-rRNA, the product of the processing reaction. In contrast, the level of the 27SB(L) pre-rRNA is not increased in the A3Δ10 mutant despite the transfer of the bulk of pre-rRNA processing to this pathway. This is probably due to cleavage in ITS2 directly on a substantial proportion of the 27SA pre-rRNA. Consistent with this, we detect a pre-rRNA which is likely to extend from C2 to A2, the predicted product of ITS2 processing on 27SA (see Figure 1A and B). In addition, a 5′ extended form of 5.8S rRNA accumulates in the A3Δ10 mutant, the hybridization pattern and gel mobility of which are consistent with its extending from the 3′ end of 5.8S rRNA to site A2. It is possible that this RNA is protected from further processing by being assembled into ribosomal subunits and transported to the cytoplasm, as is reported to occur in mutants in RNase MRP (Shuai and Warner, 1991; Lindahl *et al.*, 1992; Chu *et al.*, 1993; Schmitt and Clayton, 1993).

The essential snoRNP components are required for the early pre-rRNA cleavages at A0, A1 and A2, but do not appear to be required for A3 cleavage (see Figure 1B). What *trans*-acting factors might then be required for A3 cleavage? The effects of TS-lethal mutations and genetic depletion of the RNA component of RNase MRP have recently been reported (Shuai and Warner, 1991; Lindahl *et al.*, 1992; Chu *et al.*, 1994; Schmitt and Clayton, 1993). Like the A3Δ10 mutation, these mutants also increase the 5.8S(L):5.8S(S) rRNA ratio and accumulate a form of 5.8S rRNA extended to A2. Moreover, like the ITS1Δ3′ mutation, mutations in RNase MRP RNA result in the formation of an aberrant pre-rRNA with a 5′ end within the 18S rRNA (Shuai and Warner, 1991). It is therefore possible that RNase MRP is responsible for the cleavage at site A3, although the sequence surrounding A3 is not obviously homologous to the mitochondrial RNA sequence which was the substrate for the *in vitro* processing assay used to purify yeast RNase MRP (Stohl and Clayton, 1992). The lethality of mutations in RNase MRP has been attributed to direct effects on translation of the alteration in the 5.8S(S):5.8S(L) rRNA ratio (Shuai and Warner, 1991; Lindahl *et al.*, 1992; Schmitt and Clayton, 1993). This explanation of the phenotype seems unlikely, however, because the A3Δ10 mutants have a much greater alteration in the 5.8S(L):5.8S(S) rRNA ratio, but are not detectably impaired in growth.

The above data lead us to conclude that A3 is required *in cis* for processing at B1(S) and therefore the synthesis of the 27SB(S) pre-rRNA and 5.8S(S) rRNA. How might these two sites, which lie 76 nucleotides apart, be functionally related? One possibility is that A3 might serve as an entry site for a 5′→3′ exonuclease which digests back to B1(S). Two proteins (which we will refer to as XRN1p and RAT1p) which have 5′→3′ exonuclease activity *in vitro*, have been identified in yeast (Stevens, 1980; Larimer *et al.*, 1992; Kenna *et al.*, 1993). Moreover, *xrn1* mutants accumulate an excised fragment of the pre-rRNA consisting of the 5′ region of ITS1 from the 3′ end of 18S rRNA to A2 (Stevens *et al.*, 1991), while mutations in *RAT1* have been reported to result in the under-accumulation of 5.8S(S) (Amberg *et al.*, 1992), although in our hands the effects of *rat1-1* alone are mild. Strains doubly mutant for *RAT1* and *XRN1* have reduced processing at B1(S) and under-accumulate 5.8S(S) rRNA. These strains also accumulate 5′ extended forms of 5.8S rRNA, that extend in a ladder of bands from B1 to A3, but not beyond. Some accumulation of these RNAs is seen in *rat1* and *xrn1* single mutant strains, but the effect is very much more marked in the double mutant strain. *XRN1* is not essential for viability, and the *xrn1::URA3* mutant that we use is a null allele (Kipling *et al.*, 1991). For *RAT1*, we

used two independently isolated TS-lethal alleles, designated *rat1-1* and *tap1-1* (Aldrich *et al.*, 1993; Amberg *et al.*, 1992; Di Segni *et al.*, 1993); these show similar, although not identical, effects on A3→B1 processing, showing that the inhibition is not allele-specific. We conclude that a 5′→3′ exonuclease activity, which requires RAT1p or XRN1p, digests from site A3 to B1(S), to form the 5′ end of the 27SB(S) pre-rRNA (see Figure 1B).

In addition, *xrn1* mutant strains are impaired in a 5′→3′ exonuclease activity involved in RNA degradation (Larimer *et al.*, 1992; Hsu and Stevens, 1993), and the double mutants accumulate a number of different excised fragments of the pre-rRNA spacer regions, indicating that these proteins also have roles in the degradation of a variety of RNAs. XRN1p and RAT1p are partially homologous, consistent with the idea that they have related functions. Both genes have been isolated by several different groups, using apparently unrelated methods of selection. It seems possible that RAT1p and XRN1p function as 5′→3′ exonucleases *in vivo*; the apparent diversity of the phenotypes might arise if they were to act as the catalytic subunits of a variety of different complexes involved in RNA processing. This might be analogous to the presence of the same active protein phosphatase subunits in a number of complexes with different specificities.

The reason for the use of such a complex pathway of pre-rRNA processing is not clear. It is notable, however, that the 5′ region of 5.8S rRNA is predicted to be stably base-paired in the pre-rRNA (see Figure 1C) (Yeh *et al.*, 1990), whereas it must interact with the 25S rRNA in the mature rRNAs. The use of exonucleases to generate the major form of 5.8S rRNA has the advantage that it obligatorily renders the 5′ region of 5.8S available to base-pair with 25S rRNA. The mechanism that stops the exonucleases at the 5′ end of 5.8S rRNA is not known, but one simple model is that they are blocked by ribosomal proteins bound to the mature 5.8S domain. This mechanism would have the advantage that in the absence of correct ribosome assembly, the exonucleases would degrade the pre-rRNA, preventing the synthesis of incorrectly assembled ribosomes.

There are some clear differences between the pathways of synthesis of the 5.8S(L) and 5.8S(S) rRNAs. In pulse−chase labeling experiments, the 5.8S(L) rRNA is synthesized more rapidly than the 5.8S(S) rRNA. Since the large 27SB(L) and 27SB(S) pre-rRNAs have the same 5′ ends as the 5.8S(L) and 5.8S(S) rRNAs, the rRNAs cannot have a precursor/product relationship and their pathways of synthesis are therefore kinetically different. Moreover, in striking contrast to 5.8S(S) rRNA, the level of the 5.8S(L) rRNA is mildly increased in *rat1*; *xrn1* double mutant strains and is strongly increased in the A3Δ10 strain. This might be interpreted as indicating that the 5′ end of 5.8S(L) is formed by direct cleavage at site B1(L), which is predicted to be in a single-stranded loop in the pre-rRNA (see Figure 1C). Synthesis of 5.8S(L) is, however, kinetically delayed in *rat1*; *xrn1* strains, and the mechanism of B1(L) processing is not yet clear. Nor is it certain that the pathway of 5.8S(L) synthesis is the same in the mutant and wild-type strains.

The activities of distinct processing pathways are responsible for the 5′ heterogeneity of yeast 5.8S rRNA. In a number of other eukaryotes tested—yeasts, filamentous fungi, a higher plant, insect and vertebrates—we found a similar level of heterogeneity, suggesting that these alternative processing pathways have been conserved in eukaryotic evolution. The reason for the synthesis of the two forms of 5.8S rRNA is unclear, but it has been reported that RNase MRP mutants, which under-accumulate 5.8S(S), have an altered pattern of protein synthesis (Schmitt and Clayton, 1993), indicating that 5.8S(L) and 5.8S(S) are functionally different. We are currently testing this hypothesis.

Materials and methods

Strains and media

Growth and handling of *S.cerevisiae* were by standard techniques. Strains used are as follows. NOY504: α, *rpa12::LEU2*, *leu2-3,112*, *ura3-1*, *trp1-1*, *his3-11*, *CAN1-100* (Wittekind *et al.*, 1988) (generously provided by M.Nomura); NOY259: α, *rpa190-1*, *leu2-3,112*, *ura3-52*, *trp1-Δ1*, *his4-Δ401* (Nogi *et al.*, 1993) (generously provided by M.Nomura); DAH18: α, *rat1-1*, *leu2-Δ1*, *ura3-52*, *his3-Δ200* (Amberg *et al.*, 1992) (generously provided by C.Cole); 8-14: α, *tap1-1*, *leu1*, *ura3-1*, *ade2-1*, *lys2-1*, *met4-1*, *CAN1-100* (generously provided by B.Hall); 966-1C: **a**, *rar5::URA3*, *rat1-1*; 966-3B: α, *rar5::URA3*, *rat1-1*; 969-1C: *tap1-1*, *rar5::URA3*, *ade2-1*; 969-2B: *tap1-1*, *rar5::URA3*, *ade2-1*.

In the *xrn1::URA3* mutation the *URA3* gene is inserted 97 amino acids from the amino-terminus of the protein-coding region of the gene. No XRN1p can be detected on Western blots prepared from this strain.

Construction of pGAL::rDNA and analysis of cis-acting mutants

Construction of pGAL::rDNA involved first the insertion of a tag within 5.8S rDNA. This was achieved by replacing the 3′-most or F helix with the equivalent region of the 5.8S rDNA from *N.crassa*, substituting nucleotides 5′-CCCTTGGTATTCCAGGGG-3′ [corresponding to nucleotides 117−134 of 5.8S(S) rRNA] with 5′-TCGCCGGTATTCTG-GCGA-3′. A PCR was performed using an oligo encompassing the tag and the downstream *Sph*I site (5′-CGCTCAAACAGGCATGCTCGCCAGA-ATACTGGCGAGCGCAATGTGCGTTC-3′) together with an oligo lying upstream of the *Bsm*I site within ITS1. The PCR product was digested with *Bsm*I and *Sph*I and cloned into a pBluescript II-KS derivative containing a *Bam*HI−*Xho*I fragment of the rDNA. The ends of the latter fragment correspond to the restriction sites in the 18S rDNA tag (*Bam*HI) and 25S rDNA tag (*Xho*I) (see below). The resulting plasmid was termed pBSrDNAB-XFTag.

pGAL::rDNA was derived from pNOY102 (a generous gift from M.Nomura) in two steps. First, the *Bgl*II rDNA fragment from pNOY102 was replaced with a *Bgl*II rDNA fragment containing tags within the 18S and 25S sequences (Beltrame and Tollervey, 1992), producing pTH25. The *Sfi*I−*Xho*I fragment from pBSrDNAB-XFTag, containing the 5.8S rDNA tag, was then inserted into pTH25, creating pGAL::rDNA. The −rDNA control plasmid was produced by digesting pNOY102 with *Bam*HI and *Sal*I, filling the ends using Klenow DNA polymerase and re-ligating the plasmid on itself. This deletes the entire rDNA coding sequence.

All ITS1 deletion mutations were produced by two-step PCR. The endpoints of the deletions are indicated on Figure 1C. The PCR fragments containing the various ITS1 mutations were cloned into pBSrDNAB-XFTag: using a *Bsu*36I+*Dra*III digest for ITS1Δ5′, a *Dra*III+*Sna*BI digest for ITS1Δ3′ and a *Dra*III+*Sph*I digest for A3Δ10. *Sfi*I−*Xho*I fragments from the resulting pBSrDNAB-XFTag derivatives were then inserted into pGAL::rDNA.

We first tested whether strain NOY259 (generously provided by M.Nomura) was suitable for the analysis of rDNA mutants. This strain required prolonged growth at the non-permissive temperature for a substantial reduction in chromosomal rDNA transcription. After 24 h at 37°C, residual RNA polymerase I transcription was low enough so as not to interfere with the detection of transcripts originating from pGAL::rDNA. After such prolonged growth at the non-permissive temperature, the processing of pGAL::rDNA transcripts was, however, aberrant. We then changed to using strain NOY504 (also provided by M.Nomura). After 6 h at the non-permissive temperature, residual RNA polymerase I transcription was low enough for the clear detection of plasmid rDNA transcripts which were processed essentially identically to chromosomal transcripts from wild-type strains.

Prior to pulse−chase labeling or RNA extraction for Northern blot analysis or primer extension, NOY504 strains transformed with pGAL::rDNA or its ITS1 mutant derivatives were handled as follows: strains were grown at 23°C in minimal galactose medium until they reached mid log phase.

Cells were pelleted, resuspended in fresh minimal galactose medium, typically at an OD_{600} of 0.1, and grown for another 6 h at 37°C.

RNA extraction

RNA was extracted from exponentially growing cultures of *S.cerevisiae*, *A.nidulans* and *N.crassa*, and from young leaves of pea (*P.sativum* var. téléphone nain) as previously described (Tollervey and Mattaj, 1987). RNA was extracted from *H.wingei* and HeLa cells as described for *S.cerevisiae*. Embryos of *D.melanogaster* were disrupted by homogenization in a small volume of 4 M guanidinium thiocyanate prepared as described (Sambrook *et al.*, 1989), and extracted as described for *S.cerevisiae*. RNA was extracted from *X.laevis* oocytes by homogenizing in 'homomedium' (50 mM Tris−HCl, pH 7.5, 5 mM EDTA, 1.5% SDS, 300 mM NaCl, 1.5 mg/ml proteinase K), extracting proteins once with phenol and once with phenol/chloroform, and precipitating RNAs with 3 vols of ethanol.

Northern hybridization, primer extension and pulse−chase labeling

Northern hybridization and primer extension were performed as previously described. Oligonucleotide b is GCTCTTTGCTCTTGCC, oligonucleotide c is ATGAAAACTCCACAGTG, oligonucleotide d is CCAGTTACGA-AAATTCTTG, oligonucleotide g is GGCCAGCAATTTCAAGT and oligonucleotide e is TTTCGCTGCGTTCTTCATC. Oligonucleotide e was also used for primer extension on 5.8S rRNA from *H.wingei*, *A.nidulans*, *N.crassa* and *P.sativum*. For primer extension on 5.8S rRNA from *Drosophila*, HeLa cells and *Xenopus*, a slightly different oligonucleotide, GCTAGCTGCGTTCTTCATC, was used. Three different DNA oligonucleotides were found to hybridize poorly to the tag in the 5.8S rRNA, and oligonucleotide f was therefore synthesized from 2′-*O*-allyl RNA (Lamond and Sproat, 1993, and references therein), except for the 3′-terminal nucleotides which were deoxyribonucleotides to allow primer extension. The sequence is DGDDUDCUGGCGDdGdC, where D is 2,6-diaminopurine, which has the potential to form three hydrogen bonds to U residues (Lamm *et al.*, 1991). Oligonucleotides a and h hybridize to the tags in the 18S and 25S rRNAs respectively, and are those previously described (Beltrame and Tollervey, 1992).

For the pulse−chase labeling experiments shown in Figure 3, [^{3}H-methyl]methionine was used. This labels the methyl groups, most of which are added to the newly synthesized 35S pre-rRNA (reviewed by Klootwijk and Planta, 1989). Because of the reduced rDNA transcription of the *rpa12* strains complemented by pGAL::rDNA, there is a high lane background following pulse−chase labeling with [^{3}H]uracil, which labels all RNA species. The kinetics of pre-rRNA processing revealed by [^{3}H]uracil labeling are the same as those of wild-type strains.

[^{3}H-methyl]methionine pulse−chases were performed as described in Tollervey *et al.* (1991), except that 4 ml of cells were labeled at 37°C with 300 μCi of isotope. The methionine used for both label and chase was pre-warmed at 37°C.

Prior to the pulse−chase labeling experiment presented in Figure 9, the *rat1-1;xrn1::URA3* double mutant and wild-type strains were grown for 90 min at 37°C following a gradual increase of temperature from 23°C to 37°C. [^{3}H]uracil pulse−chase was then performed as described (Tollervey *et al.*, 1991), except that 6 ml of cells were labeled at 37°C with 150 μCi of isotope. The uracil used for both label and chase was pre-warmed at 37°C.

Depletion of snoRNP components

The depletion of U3, U14, snR30, SOF1p, NOP1p and GAR1p under the control of *GAL* promoters has previously been reported (Li *et al.*, 1990; Hughes and Ares, 1991; Tollervey *et al.*, 1991; Girard *et al.*, 1992; Jansen *et al.*, 1993; Morrissey and Tollervey, 1993).

Acknowledgements

We would like to thank the following for generously making material available; the group of Masayasu Nomura for pNOY102 and strains NOY504, NOY505 and NOY259, Charles Cole and David Amberg for the *rat1-1* strain and the group of Ben Hall for the *tap1-1* strain. We would also like to thank Phil Mitchell, Bertrand Séraphin and Iain Mattaj for critical reading of the manuscript. S.K. was partially supported by a grant from the Cancer Research Campaign.

References

Aldrich,T.L., Di Segni,G., McConaughy,B.L., Keen,N.J., Whelen,S. and Hall,B.D. (1993) *Mol. Cell. Biol.*, **13**, 3434−3444.

Amberg,D.C., Goldstein,A.L. and Cole,C.N. (1992) *Genes Dev.*, **6**, 1173−1189.

Beltrame,M. and Tollervey,D. (1992) *EMBO J.*, **11**, 1531−1542.

Brand,R.C., Klootwijk,J., van Steenbergen,T.J.M., de Kok,A.J. and Planta,R.J. (1977) *Eur. J. Biochem.*, **75**, 313−318.

Chang,D.D. and Clayton,D.A. (1987a) *Science*, **235**, 1178−1184.

Chang,D.D. and Clayton,D.A. (1987b) *EMBO J.*, **6**, 409−417.

Chu,S., Archer,R.H., Zengel,J.M. and Lindahl,L. (1994) *Proc. Natl Acad. Sci. USA*, **91**, 659−663.

Di Segni,G., McConaughy,B.L., Shapiro,R.A., Aldrich,T.L. and Hall,B.D. (1993) *Mol. Cell. Biol.*, **13**, 3424−3433.

Girard,J.P., Lehtonen,H., Caizergues-Ferrer,M., Amalric,F., Tollervey,D. and Lapeyre,B. (1992) *EMBO J.*, **11**, 673−682.

Hsu,C.L. and Stevens,A. (1993) *Mol. Cell. Biol.*, **13**, 4826−4835.

Hughes,J.M.X. and Ares,M.J. (1991) *EMBO J.*, **10**, 4231−4239.

Jansen,R., Tollervey,D. and Hurt,E.C. (1993) *EMBO J.*, **12**, 2549−2558.

Kearsey,S. and Kipling,D. (1991) *Trends Cell Biol.*, **1**, 110−112.

Kenna,M., Stevens,A., McCammon,M. and Douglas,M.G. (1993) *Mol. Cell. Biol.*, **13**, 341−350.

Kipling,D., Tambini,C. and Kearsey,S.E. (1991) *Nucleic Acids Res.*, **19**, 1385−1391.

Kiss,T., Marshallsay,C. and Fillipowicz,W. (1992) *EMBO J.*, **11**, 3737−3746.

Klootwijk,J. and Planta,R.J. (1989) *Methods Enzymol.*, **180**, 96−109.

Lamm,G.M., Blencowe,B.J., Sproat,B.S., Iribarren,A.M., Ryder,U. and Lamond,A.I. (1991) *Nucleic Acids Res.*, **19**, 3193−3198.

Lamond,A.I. and Sproat,B.S. (1993) *FEBS Lett.*, **325**, 123−127.

Larimer,F.W., Hsu,C.L., Maupin,M.K. and Stevens,A. (1992) *Gene*, **120**, 51−57.

Li,H.V., Zagorski,J. and Fournier,M.J. (1990) *Mol. Cell. Biol.*, **10**, 1145−1152.

Lindahl,L., Archer,R.H. and Zengal,J.M. (1992) *Nucleic Acids Res.*, **20**, 295−301.

Maden,B.E.H. (1990) *Prog. Nucleic Acids Res. Mol. Biol.*, **39**, 241−303.

Morrissey,J.P. and Tollervey,D. (1993) *Mol. Cell. Biol.*, **13**, 2469−2477.

Musters,W., Venema,J., van der Linden,G., van Heerikhuizen,H., Klootwijk,J. and Planta,R.J. (1989) *Mol. Cell. Biol.*, **9**, 551−559.

Musters,W., Boon,K., van der Sande,C.A.F.M., van Heerikhuizen,H. and Planta,R.J. (1990) *EMBO J.*, **9**, 3989−3996.

Nogi,Y., Yano,R. and Nomura,M. (1991) *Proc. Natl Acad. Sci. USA*, **88**, 3962−3966.

Nogi,Y., Yano,R., Dodd,J., Carles,C. and Nomura,M. (1993) *Mol. Cell. Biol.*, **13**, 114−122.

Reddy,R., Li,W.-Y., Henning,D., Choi,Y.C., Nohga,K. and Busch,H. (1981) *J. Biol. Chem.*, **256**, 8452−8457.

Reddy,R., Henning,D. and Busch,H. (1985) *J. Biol. Chem.*, **260**, 10930−10935.

Sambrook,J., Fritsch,E.F. and Maniatis,T. (1989) *Molecular Cloning. A Laboratory Manual.* 2nd edn. Cold Spring Harbor Laboratory Press, Cold Spring Harbor, NY.

Schmitt,M.E. and Clayton,D.A. (1992) *Genes Dev.*, **6**, 1975−1985.

Schmitt,M.E. and Clayton,D.A. (1993) *Mol. Cell. Biol.*, **13**, 7935−7941.

Shuai,K. and Warner,J.W. (1991) *Nucleic Acids Res.*, **19**, 5059−5064.

Stevens,A. (1980) *J. Biol. Chem.*, **255**, 3080−3085.

Stevens,A., Hsu,C.L., Isham,K.R. and Larimer,F.W. (1991) *J. Bacteriol.*, **173**, 7024−7028.

Stohl,L. and Clayton,D.A. (1992) *Mol. Cell. Biol.*, **12**, 2561−2569.

Tollervey,D. and Mattaj,I.W. (1987) *EMBO J.*, **6**, 469−476.

Tollervey,D., Lehtonen,H., Carmo-Fonseca,M. and Hurt,E.C. (1991) *EMBO J.*, **10**, 573−583.

Udem,S.A. and Warner,J.R. (1972) *J. Mol. Biol.*, **65**, 227−242.

van der Sande,C.A.F.M., Kwa,M., van Nues,R., van Heerikhuizen,H., Raué,H.A. and Planta,R.J. (1992) *J. Mol. Biol.*, **223**, 899−910.

Veldman,G.M., Brand,R.C., Klootwijk,J. and Planta,R.J. (1980) *Nucleic Acids Res.*, **8**, 2907−2920.

Veldman,G.M., Klootwijk,J., van Heerihuizen,H. and Planta,R.J. (1981) *Nucleic Acids Res.*, **19**, 4847−4862.

Wittekind,M., Dodd,J., Vu,L., Kolb,J.M., Buhler,J.-M., Sentenac,A. and Nomura,M. (1988) *Mol. Cell. Biol.*, **8**, 3997−4008.

Yeh,L.-C.C., Thweatt,R. and Lee,J.C. (1990) *Biochemistry*, **29**, 5911−5918.

Yuan,Y., Singh,R. and Reddy,R. (1989) *J. Biol. Chem.*, **264**, 14835−14839.

Received on January 14, 1994; revised on February 25, 1994